Electronic Supplementary Material (ESI) for Chemical Science.
This journal is © The Royal Society of Chemistry 2020

Supporting information

Sodium Caseinate as a Particulate Emulsifier for Making Indefinitely Recycled pH-Responsive Emulsions

Yongkang Xi,[a] Bo Liu,[a] Hang Jiang,[b] Shouwei Yin,*[a b, c] To Ngai*[b] and Xiaoquan Yang[a, c]

[a] Research and Development Centre of Food Proteins, School of Food Science and Engineering, and Guangdong Province Key Laboratory for Green Processing of Natural Products Safety, South China University of Technology, Guangzhou, 510640, P. R. China.

[b]Department of Chemistry, The Chinese University of Hong Kong, Shatin, N. T., Hong Kong.

[c]Overseas Expertise Introduction Center for Discipline Innovation of Food Nutrition and Human Health (111 Center), Guangzhou 510640, PR China

*Corresponding authors:

*Yin, S. W. E-mail: feysw@scut.edu.cn

*Ngai, T. E-mail: tongai@cuhk.edu.hk

Table of Contents

Experimental Procedures

Materials.

NaCas was provided by Zhengzhou Taber Trading Co. Ltd. Chloroauric acid trihydrate ($HAuCl_4 \cdot 3H_2O$, 47% Au base) was purchased from Aladdin Chemical Reagent Company (Shanghai, China). Ethyl acetate, sodium borohydride ($NaBH_4$) and p-nitroanisole were obtained from Lanzhou Institute of Chemical Physics (Lanzhou, China). Zein (product Z 3625), BSA and silica (LUDOX TM-50) were purchased from Sigma Chemical Co. (St. Louis, MO, USA). Gelatin was purchased from Beijing Dingguo Changsheng Biotechnology Co. Ltd (Beijing, China). WPI (NZMP) was purchased from Fonterra (New Zealand). SPI was extracted by previous report.[1] Sericin was obtained by previous report.[2] Fluorescent dyes including Nile Red, Nile Blue A, and fluoresceine 5(6)-isothiocyanate mixed isomers (FITCs) were obtained from Sigma-Aldrich, Inc. (St. Louis, MO, USA). All other chemicals were of analytical grade.

pH-Responsive Performance of NaCas.

To investigate the pH-responsiveness of NaCas in aqueous solution, 5 mg of NaCas was dispersed in 10 mL of deionized water. The solution was repeatedly adjusted to pH 8.0 and 5.1 by the addition of 0.01 M HCl and 0.01 M NaOH. The light transmittance and morphology of the NaCas solutions were monitored throughout the cycle. The pH of the NaCas solution was gradually adjusted to 4.95, and the morphology of NaCas was monitored using TEM or SEM. In addition, the agglomerates (at pH 5.1) were further diluted to 0.01 wt% using an aqueous solution at pH 5.1, and the dissociated micelle morphology was characterized using TEM or SEM.

In brief, TEM observations were performed using a JEM-1400 Plus (JEOL Ltd, Japan) at an acceleration voltage of 120 kV. The sample (0.005-0.05 wt%) was dispersed in deionized water, and the pH of the solution was adjusted to 8.00, 5.10, or 4.95. A drop of the dispersion was spread onto 300 mesh copper grids coated with a carbon support film, and the specimens were then dried under vacuum for one day. In addition, a drop of phosphotungstic acid was added to stain NaCas for easy observation.

Morphological observations were also performed using a Merlin scanning electron microscope (Zeiss Co., Germany). The samples were dispersed in deionized water (0.05 wt%) under mechanical agitation at 600 rpm for 2 min. One drop of the dispersion was carefully placed on a glass slide and dried at room temperature. After that, the samples were coated with Au for conductivity and placed under the microscope for observation.

pH-Responsive Performance of Emulsions Stabilized by NaCas.

Typically, 10 mL of oil phase and 10 mL of a NaCas suspension (0.1 wt%) were mixed in 25 mL glass vessels at room temperature. Emulsions were formed using an Ultraturrax T10 homogenizer (IKA, Germany) at a stirring rate of 15 000 rpm for 1 min. After standing at room temperature for 30 min, a few drops of HCl were added to adjust the pH to 4.6-5.0 to break up the emulsion. Slight magnetic stirring, stick stirring or hand shaking was used to facilitate the demulsification of the emulsions (Supplementary Movie 1, 2 and 3). Finally, the cyclability of the NaCas-stabilized emulsions was assessed with a saturated salt solution (NaCl ~ 6.1 M) or seawater (containing mixed ions) used as the solvent. The morphology of the emulsion was characterized using an optical microscope, a laser confocal microscope and a cryo-electron microscope.

To verify the uniqueness of the pH-responsive NaCas-stabilized emulsions, we constructed a series of emulsions using 6 representative proteins, including three animal proteins (BSA, WPI, gelatin), two plant proteins (SPI and zein), and an insect protein (sericin), and the pH-triggered cyclability of the emulsions were investigated. In addition to zein, the pH-triggered cycle was performed using the abovementioned procedure for NaCas-stabilized emulsions. ZCPs were prepared as a particulate emulsifier by an anti-solvent protocol. Typically, 10 mL of oil phase and 10 mL of a ZCP dispersion (0.1 wt%, pH 3.0) were mixed in 25 mL glass vessels at room temperature, and the mixture was sheared using an Ultraturrax T10 homogenizer at a stirring rate of 15 000 rpm for 1 min. After incubation at room temperature for 30 min, a few drops of NaOH was added to adjust the pH to 4.6-7.0 to break up the emulsions.

Cryo-SEM measurements were performed on a Hitachi S-4800 instrument operating at 2.0 kV. Samples (emulsions) were frozen with liquid nitrogen and sublimated for 10 min at −90 °C to expose the sample structure. The surface of the sample was removed with a blade to facilitate observation of the interfacial structure and immediately measured.

CLSM images were recorded on a Leica TCS SP5 confocal laser scanning microscope (Leica Microsystems Inc., Heidelberg, Germany) equipped with a 20-HC PL APO/0.70NA oil-immersion objective lens. The samples were stained with a mixture of Nile blue (0.1%) and Nile red (0.1%). The stained samples were placed on concave confocal microscope slides and examined using a 630x magnification lens. The two dyes were excited with an argon/krypton laser and a helium/neon (He-Ne) laser at 488 nm and 633 nm, respectively.

An optical contact angle meter (OCA-20) with oscillating drop accessory ODG-20 (Dataphysics Instruments GmbH, Germany) was used to measure the adsorption kinetics of NaCas solution at pH 8.0 and pH 4.8 (0.5

mg mL^{-1}). A drop of NaCas solution (10 μL) was delivered by an inverted tip of syringe into an optical glass cuvette containing purified oil, and allowed to stand for 3 h to achieve adsorption at the oil-water interface. The drop image was photographed using the high-speed video camera, and the interfacial tension (γ) was calculated from the drop shape by Young–Laplace equation, as described in Güzey, Gülseren, Bruce, and Weiss (2006) [3]. All the measurements were performed in duplicates at a room temperature of 25 °C. For each sample two consecutive measurements were performed, and each sample was replicated at least 2 times.

Simulated seawater (SW) was prepared according to ASTM International standard D1141. Salt media included sodium chloride (NaCl, 24.53 g L^{-1}), magnesium chloride ($MgCl_2$, 5.2 g L^{-1}), sodium bicarbonate ($NaHCO_3$, 0.201 g L^{-1}), sodium sulfate (Na_2SO_4, 4.09g L^{-1}) , calcium chloride ($CaCl_2$, 1.16 g L^{-1}), hydrochloric acid (HCl, 0.695 g L^{-1}), potassium bromide (KBr, 0.101g L^{-1}), boric acid (H_3BO_3, 0.027 g L^{-1}), strontium chloride ($SrCl_2$, 0.025 g L^{-1}) and sodium fluoride (NaF, 0.003 g L^{-1}). The pH of as-prepared simulated seawater was adjusted to 8.2 using 0.1 M NaOH solution.

NaCas synergistic nanoparticle to construct pH response emulsion.

NaCas-zein particles were prepared using a modified method based on antisolvent procedure. In brief, zein (1.0 g) was dissolved in 40 mL 80% ethanol solvent (v/v) at room temperature to form a stock solution. The zein stock solution was added drop-wise into 120 mL 0.083% NaCas solution under vigorous stirring in 10 minutes. After that, the remained ethanol in the dispersions was removed under reduced pressure by rotary evaporation. Finally, the concentration of NaCas-zein in the particle dispersions was 1.8 % (w/v). The particle dispersions were stored in 5 °C.

For easy observation, the Pickering emulsion was solidified by copolymerization reaction. The procedure was the same as that of traditional Pickering emulsion, except 0.56 wt % of AIBN, 1.4 wt % styrene, and 2.1 wt % divinylbenzene (DVB) was dissolved in 1 mL of n-heptane prior to emulsification. Then, the resulting emulsion was poured into a 10 mL plastic vessel and deoxygenated with N_2 for 20 min. The reaction mixture was heated to 65 °C and subsequently polymerized for 16 h. During this process, hollow polystyrene microcapsules were formed as the n-heptane was a poor solvent for the cross-linked polystyrene network, leading to phase separation and precipitation at the oil/water interface, locking the stabilizers into the capsule surface (polystyrene layer). Therefore, we could speculate the location of stabilizers at the actual oil–water interface by observing them at the polystyrene layer in the hollow microcapsules.

Fluorescent Tagging of Zein. Briefly, zein (3 g) were dissolved in 100 mL DMF under stirring. Then, the solution added 0.1 mL of triethylamine and 80 mg of FITC at room temperature and reacted for 24h with stirring. The solution was washed using dichloromethane (DCM) (50 mL) and separated the fractions. The process was repeated for six times to ensure that all free dye was removed. The final suspension was dried in an oven (40 °C) under high vacuum for 24 h to remove remaining organic solvents. FITC labeled-silica. Silica (1g) dissolved in 10 mL deionized water. The solution added 1mL FITC (1 mg/mL, dissolve in DMSO) solution at 40 °C. After stirring for 24h, the solution was washed using ethanol and deionized water for six times to remove the free dye. The final suspension was freeze dryed for 48h to obtain FITC labeled-silica.

Synthesis of Au-loaded NaCas (NaCas-Au NCs).

Au NCs were deposited on NaCas through the reduction of $HAuCl_4$ by $NaBH_4$ according to the method of Mahmoud et al[4] with some modifications. In brief, $HAuCl_4 \cdot 3H_2O$ (10 mM, 1 mL) was added to 50 mL (0.2 wt%, pH 7.0) of a NaCas suspension, and then 0.5 mL aliquots of freshly prepared ice-cold 10 mM $NaBH_4$ were added slowly to the mixing suspension until a stable brown-yellow colloid was observed (2.5 mL of $NaBH_4$). The suspension was left at room temperature for 24 h for stabilization. Au NP-labelled NaCas was isolated by adjusting the pH to 4.7 and then centrifuging at 5000 rpm. The sediment was washed with deionized water until the supernatant was clear. After freeze-drying, the product was obtained.

Physicochemical Characterization of NaCas-Au NCs.

TEM observations were performed using a JEM-2100 Plus (JEOL Ltd, Japan) at an acceleration voltage of 200 kV. The sample (0.05 wt%) was dispersed in deionized water and homogenized at 25 °C for 5 min. A drop of the suspension was spread onto copper grids coated with a carbon support film. After 1 min, excess liquid was blotted with filter paper, and the remaining film was allowed to dry for observation.

Atomic force microscopy (AFM) images were acquired on a Bruker Multimode instrument with a Quadrexed Nanoscope 3D controller. Samples were prepared by adding one drop of proteinosome solution (0.02 wt%) onto a clean silica wafer and drying under vacuum for one day.

XPS spectra were recorded on a Kratos Axis Ultra DLD instrument, and the C_{1S} line at 284.6 e V was used as a reference.

The FT-IR spectra of the samples were recorded using a Perkin Elmer Spectrum RXIFT-IR Spectrometer

(USA) at room temperature. The sample powder was blended with KBr powder and pressed into tablets before spectra were obtained over the range of 4000 to 500 cm^{-1} at a resolution of 8 cm^{-1}.

The UV-Vis spectra of Au NCs-NaCas was recorded by Nano Photometer N60 instrument (IMPLEN, Germany).

XRD data of the samples were obtained with a RU200R X-ray diffractometer (Rigaku, Tokyo, Japan) by using Cu Kα radiation at 35 kV and 20 mA, a theta-compensating slit, and a diffracted beam monochromator in a range of 2θ = 25−65°.

Au and P content were analyzed with an inductively coupled plasma-atomic emission spectrometry (ICP-AES, Atom Scan16, TJA Co.). An aliquot of sample (10 mg) was taken, and 5 mL of nitric acid and 1 mL of hydrogen peroxide were added, and the mixture was heated on a hot plate at 300 °C for digestion.

Preparation and Characterization of Emulsions Stabilized by NaCas-Au NCs.

Typically, 10.0 mL of oil phase and 10.0 mL of NaCas-Au NC suspensions (1 mg/mL) were mixed in 25 mL glass vessels at room temperature. Emulsions were formed using an Ultraturrax T10 homogenizer (IKA, Germany) at a stirring rate of 15 000 rpm for 1 min.

CLSM images were recorded on a Leica TCS SP5 confocal laser scanning microscope (Leica Microsystems Inc., Heidelberg, Germany) equipped with a 20-HC PL APO/0.70NA oil-immersion objective lens. The samples were stained with Nile red (0.1%). The stained samples were placed on concave confocal microscope slides and examined using a 630x magnification lens. The dye was excited with an argon/krypton laser and a He-Ne laser at 488 nm.

Catalytic reaction.

Ethyl acetate (10 mL) containing p-nitroanisole (4 mM) and NaCas-Au NCs aqueous solution (10 mL) were added to a clean plastic vial at room temperature. Then, a few drops of NaOH solution (1 M) were added into this system to adjust the pH to 8.0-8.5. Emulsions were formed by homogenization using an Ultraturrax T10 homogenizer (IKA, Germany) at a stirring rate of 15 000 rpm for 1 min. Excess $NaBH_4$ aqueous solution was added to the emulsions with gentle stirring. Hydrogenation was conducted under stirring at room temperature for a given time. After the reaction, a known volume of HCl (1 M) aqueous solution was added to the emulsion to break it up. After complete phase separation, the resulting extra upper oil phase was carefully isolated by

decantation. The yield was determined with a 7890B gas chromatograph (Agilent Technologies Co., China). For the next reaction cycle, fresh solvent and substrate were added to the residual water phase. A few drops of NaOH solution were added to the above system to adjust the pH to the basic range. After homogenization, emulsions stabilized by NaCas-Au NCs formed again. The other procedures for the reaction and catalyst recycling were the same as those used in the first reaction cycle.

Results and Discussion

Reversible pH-responsive association-disassociation of NaCas

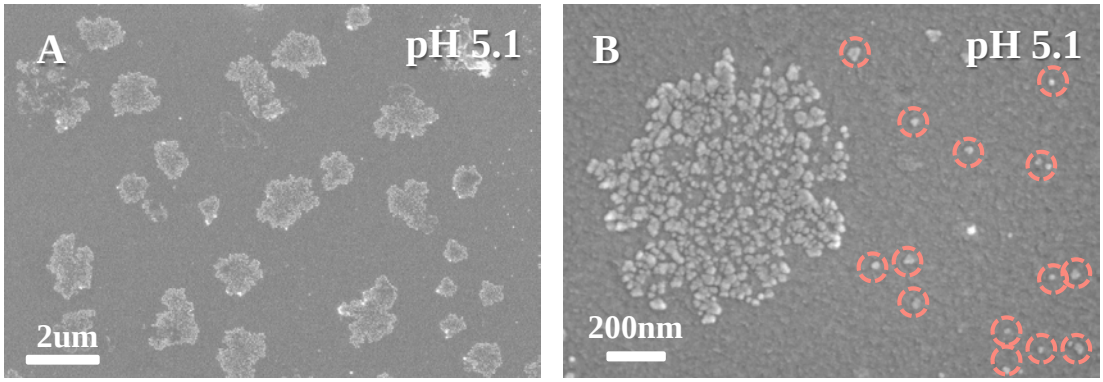

Fig. S1 SEM images of NaCas (0.01 wt%). NaCas was diluted by 5 times from 0.05 wt% to 0.01 wt% by magnetic stirring, and the pH of NaCas solution remained constant (pH 5.1). Interestingly, the intermediate colloidal architecture at pH 5.1 returned to the uniformed sub-micelles with particle size of 20-40 nm after the dilution by 5 times

pH-responsive emulsions stabilized by NaCas

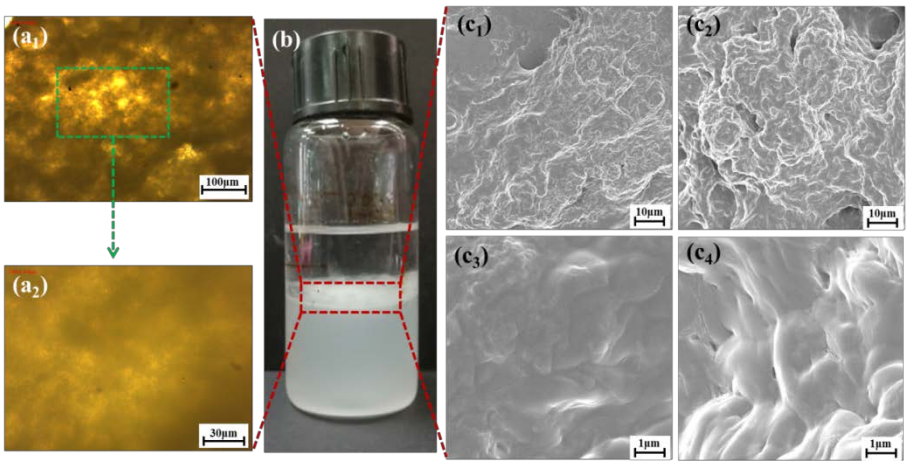

Fig. S2 Optical micrographs, photograph and SEM of flocs between oil and water layers after demulsification for the 1st cycle (a_1, a_2, b, c_1, c_3) and 10th cycle (c_2, c_4). Lipid droplets were not observed in flocs using the optical microscope and SEM , and the agglomerates between the ethyl acetate and water layers detected after demulsification were flocs of NaCas after the first and tenth cycles.

Universality and potential applications of this strategy

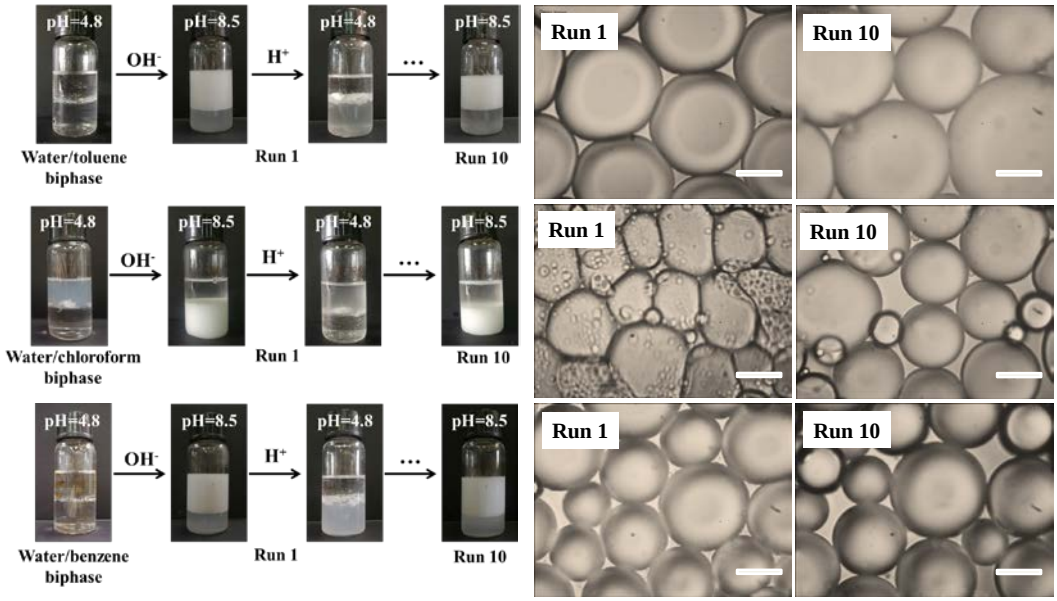

Fig. S3 Responsiveness of NaCas-stabilized emulsions with different oil phase. The appearance and selected microscopic images for the successive pH-triggered NaCas-stabilized emulsion inversion using toluene, chloroform and benzene as oil phase, respectively. Scale bar, 30 μm.

Specificity of pH-responsive emulsions stabilized by NaCas

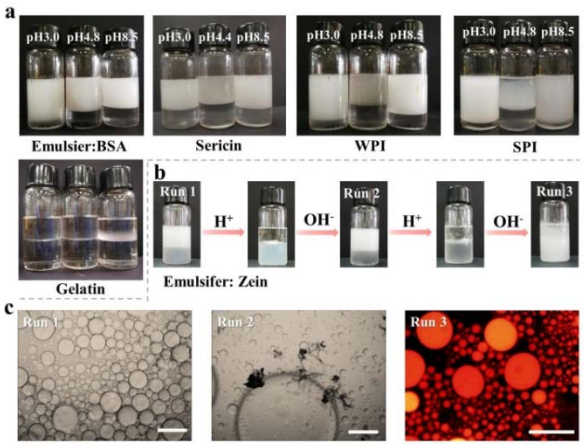

Fig. S4 pH-responsive behaviour of emulsions stabilized by different types of proteins. (a) Appearance of emulsions stabilized by BSA, sericin, WPI, SPI, and gelatin at a protein concentration of 0.1 wt% using ethyl acetate as the oil phase. (b, c) Appearance and optical micrographs of successive pH-responsive conversion cycles of emulsions stabilized by ZCPs (0.1 wt%) using ethyl acetate as the oil phase (1st, 2nd and 3rd cycle). In the 2nd cycle of emulsification/demulsification, some insoluble zein aggregates appeared around the emulsion droplets. In the 3rd cycle, the emulsion remained in the oil-in-water state, but oil leakage happened. Scale bar, 100 μm. Two points make casein special: (1) Casein is a family of intrinsically disordered proteins (IDPs) and has almost no folded or secondary structure with a high proportion of accessible non-polar residues, thereby implying a strong tendency to aggregate or flocculate at the vicinity of isoelectric point. Casein includes αs1- and αs2-caseins (collectively called α-casein), β-casein, and κ-casein. αs1-casein is a triblock copolymer, and monomeric β-casein and κ-casein have both hydrophobic and hydrophilic extremities. (2) Casein proteins in milk are phosphorylated at clusters of serine residues in relatively close proximity in the primary structure. Caseins have a number of Ser (P) residues in specific phosphorylation-site motifs, such as [-(Ser(P)-)3 (Glu-)2].[5-7] NaCas is derived from casein and has a highly disordered structure. When the pH was shifted to neutral or alkaline values, deprotonation of the phosphoserine clusters inside the agglomerates made them highly negatively charged. Such electrostatic repulsion should lead to the agglomerates to disperse into a sub-micelle state. This is why the NaCas-stabilized emulsion can be formed and broken within 1 min. Furthermore, the phosphoserine clusters can dynamically bind to the positive ions to form a positively charged layer around the localized micelles, serving as a vehicle for capturing ions,[8-10] and providing theoretical support for strong salt tolerance, and thus contributing to the indefinitely reversible pH-responsive cyclability that cannot be found in other common proteins.

Working principle for pH-responsive emulsions stabilized by NaCas

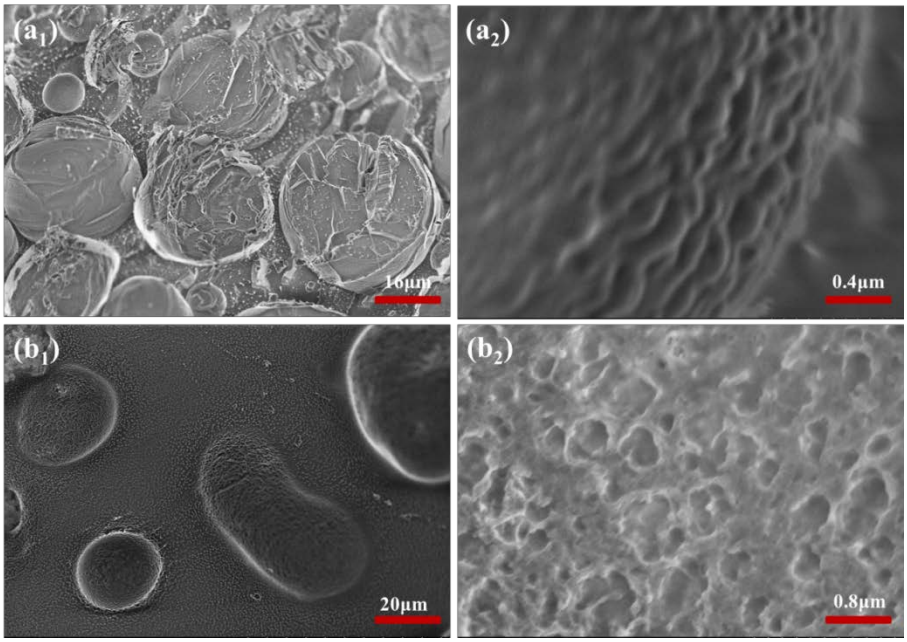

Fig. S5 Cryo-SEM images of NaCas-stabilized emulsions at pH 8.0 (a_1, $a_{2)}$ and 4.8 (b_1, b_2) using dodecane as oil phase.

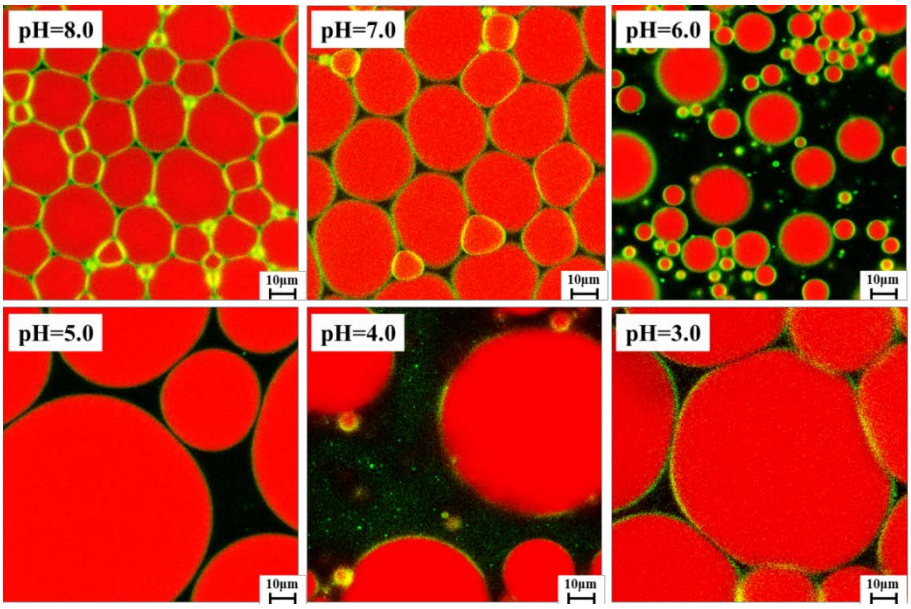

Fig. S6 CLSM images of NaCas stabilized emulsions at different pH values using dodecane as oil phase. Red fluorescence from Nile Red (dodecane) lay in the spherical droplets, and there were obvious green circles (NaCas) around spherical droplets. The thickness of the interfacial protein layers decreased, and aggregates of NaCas appeared in the aqueous phase as the pH was shifted to 5.0 and 4.0.

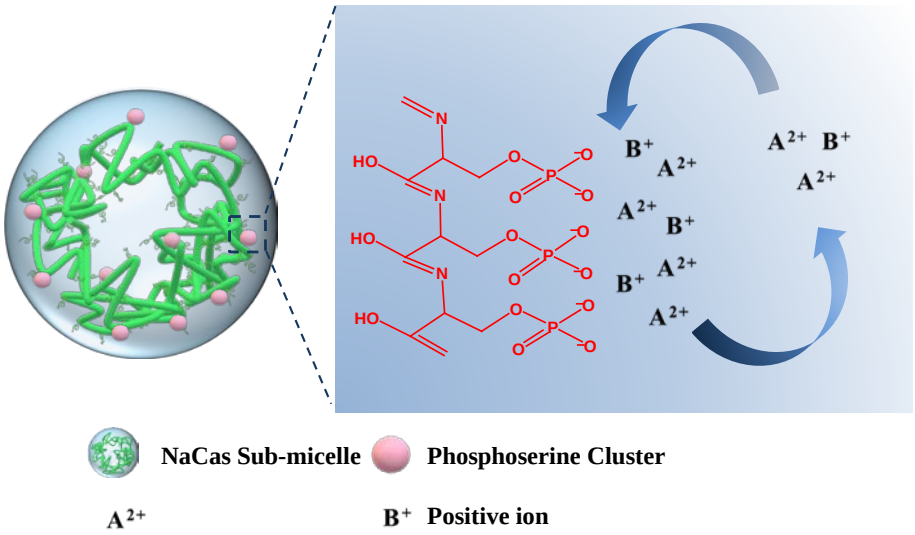

Fig. S7 Schematic representation of possible mechanisms for salt tolerance of NaCas. Casein includes αs1- and αs2-caseins (collectively called α-casein), β-casein, and κ-casein. The αs1-, αs2-, and β-caseins undergo extensive phosphorylation on their serine residues and form the phosphate centers (phosphoserine clusters). These caseins have a number of Ser (P) residues in specific phosphorylation-site motifs, such as [-(Ser(P)-)3 (Glu-)2], which give them a high sequestering power towards divalent metal ions for example Ca^{2+}, $Mg^{2+}$and Cu^{2+}.[11, 12] The phosphoserine cluster dynamically binds to the positive ion, that is, the phosphoserine cluster and the positive valence ion are always in the dissociation-binding dynamic state, so a large amount of positive valence ions are enriched around the protein, which may form a positively charged layer around the localized micelle. And strong charge repulsion is beneficial for protein dispersion. Casein phosphopeptides (CPP) derived from casein by tryptic digestion were routinely used to sequester and enhance Ca^{2+} absorption as a viable functional ingredient in food industry,[13] providing practical support for strong salt tolerance, and thus contributing to the indefinitely reversible pH-responsive cyclability that cannot be found in other common proteins.

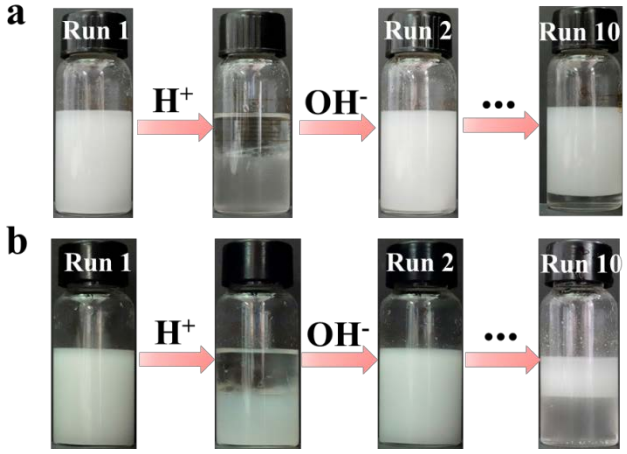

Fig. S8 pH-responsive emulsions stabilized by SiO_2-NaCas and zein-NaCas. Appearance of successive pH-responsive SiO_2-NaCas stabilized emulsion (0.004 wt% NaCas and 0.02wt% SiO_2) conversion cycles using ethyl acetate as the oil phase (1st and 10th cycle). (b) Appearance of successive pH-responsive zein-NaCas stabilized emulsion (0.1 wt% NaCas-zein) conversion cycles using ethyl acetate as the oil phase (1st and 10th cycle).

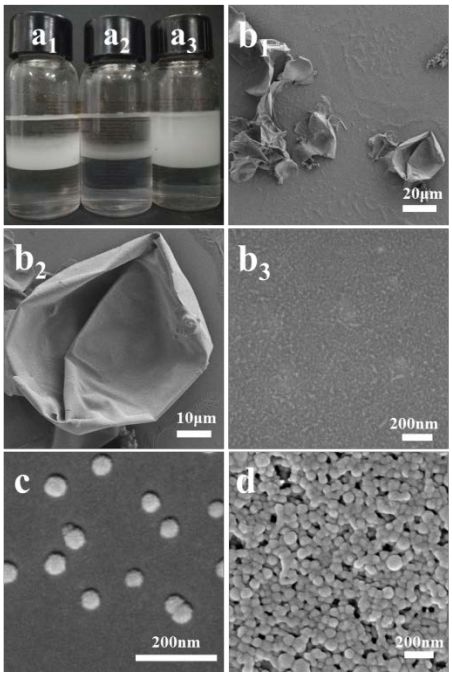

Fig. S9 The appearance of emulsion stabilized by NaCas (a_1, 0.004wt%), SiO_2 (a_2, 0.02wt%) and SiO_2-NaCas (a_3, 0.004wt% NaCas and 0.02wt% SiO_2) using ethyl acetate as oil phase. (b_1-b_3) SEM images of NaCas-stabilized emulsions at pH 8.0. (c-d) SEM images of SiO_2 (c) and zein-NaCas (d).

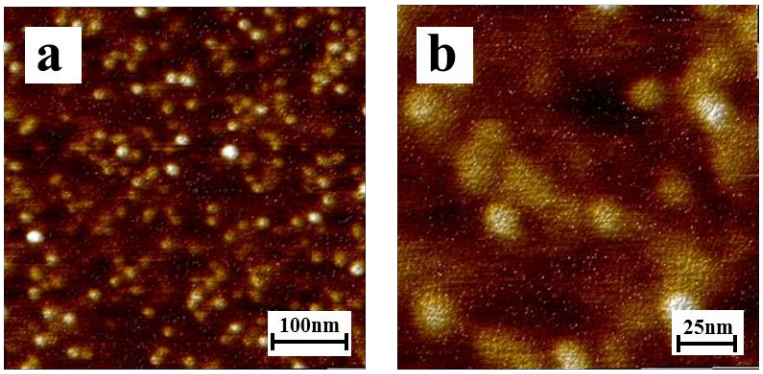

Fig. S10 AFM images of NaCas-Au NCs at pH 8.0. b is a partial enlarged view of a.

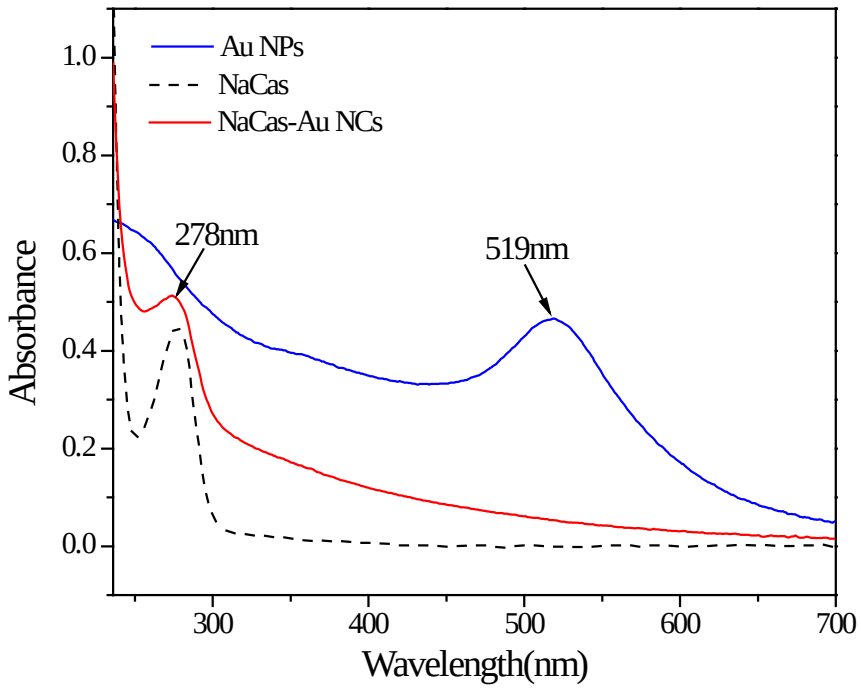

Fig. S11 UV−visible spectra of Au NPs, NaCas and NaCas-Au NCs. The maximum UV-vis absorbance at 278 nm belongs to NaCas, and the gold nanoparticles has an absorption peak at 519 nm.

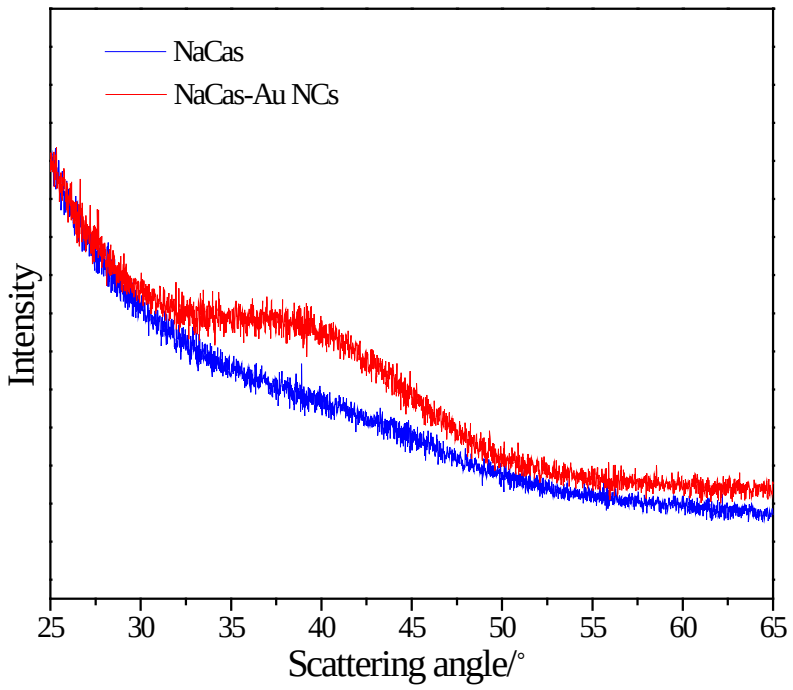

Fig. S12 XRD spectra of the NaCas and NaCas-Au NCs.

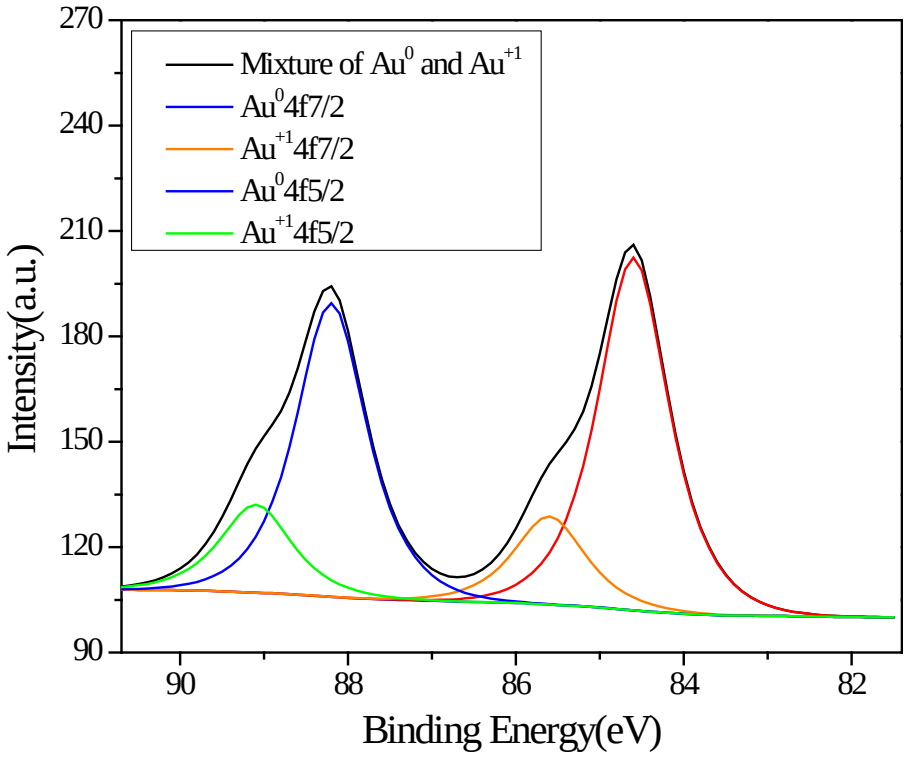

Fig. S13 XPS spectra of the NaCas-Au NCs.

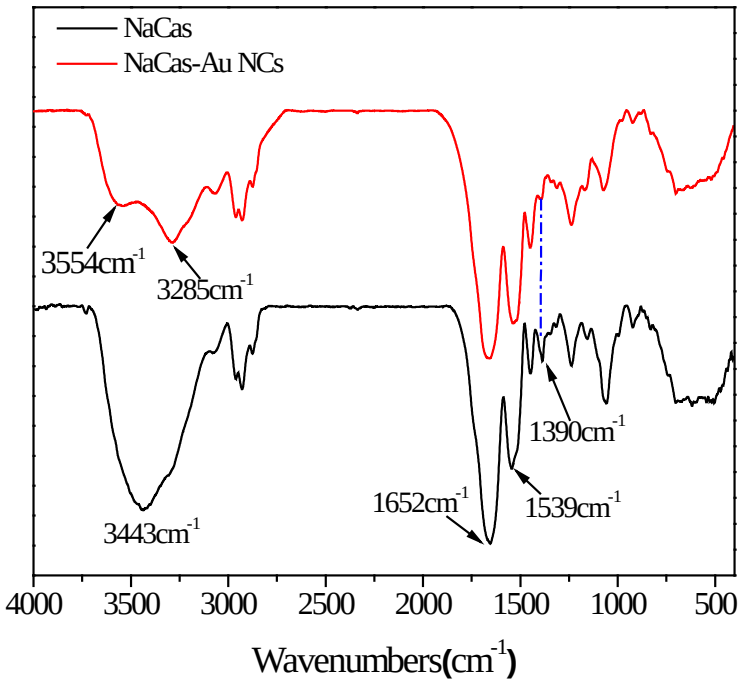

Fig. S14 FTIR spectra of the NaCas and NaCas-Au NCs. We hence investigated the variation in functional groups using Fourier transform infrared (FT-IR) spectroscopy. Pure NaCas showed a stretching vibration peak corresponding to the N−H bond at 3443 cm-1 and displayed three peaks at 1652 cm-1 (C=O stretching), 1539 cm-1 (N–H bending) and 1390 cm-1 (C–N stretching).[14] However, the peak at 1390 cm^{-1} weakened after binding NaCas to Au NCs, most likely because the amide bonds in the NaCas-Au NCs are not infrared active. This feature has been reported for amide bonds in GSH-protected nanoclusters. We also verified that the stretching vibration peak of the N−H bond at 3000−3500 cm-1 shifted to a higher frequency than the corresponding peak in the spectrum of NaCas.[15]

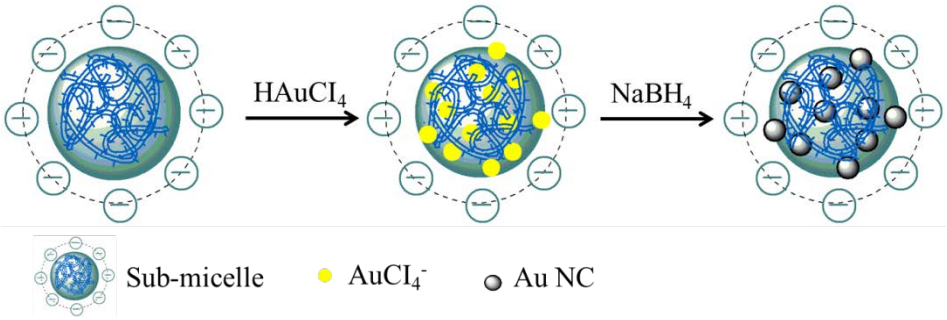

Fig. S15 Schematic representation of possible mechanisms for the formation of NaCas-Au NCs

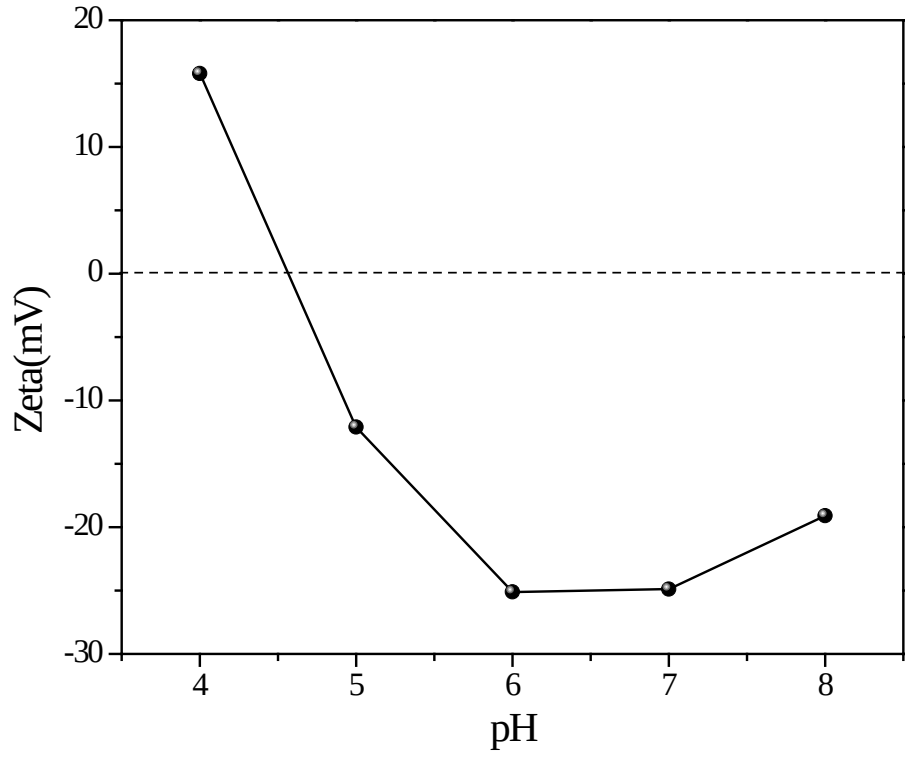

Fig. S16 Zeta potential of NaCas-Au NCs (0.5 mg mL^{-1}) as a function of pH values.

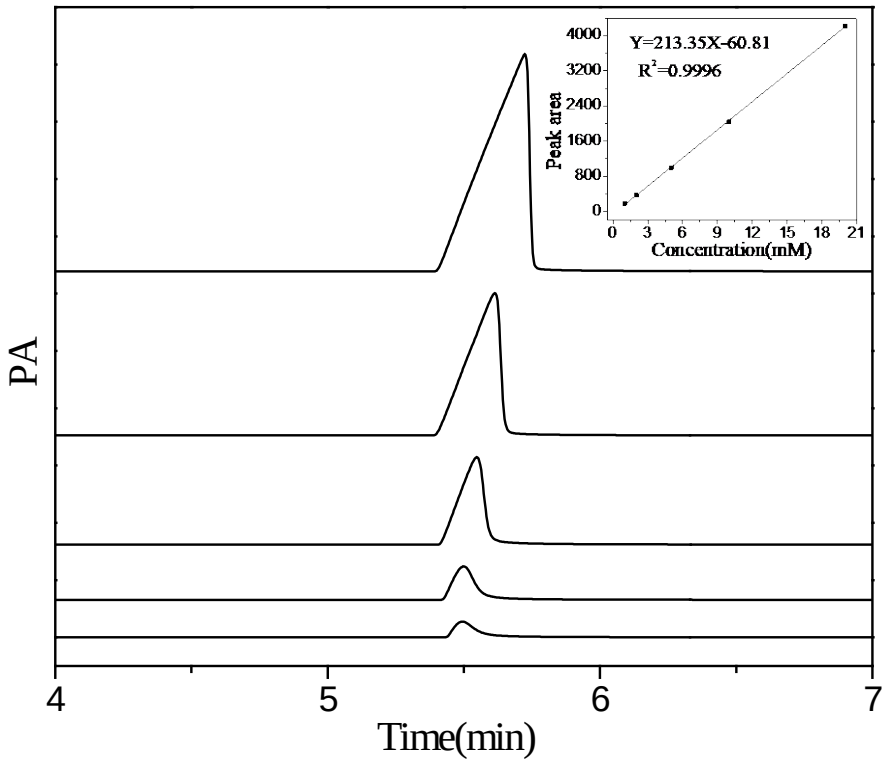

Fig. S17 Gas chromatograms (GC) of p-nitroaniline.

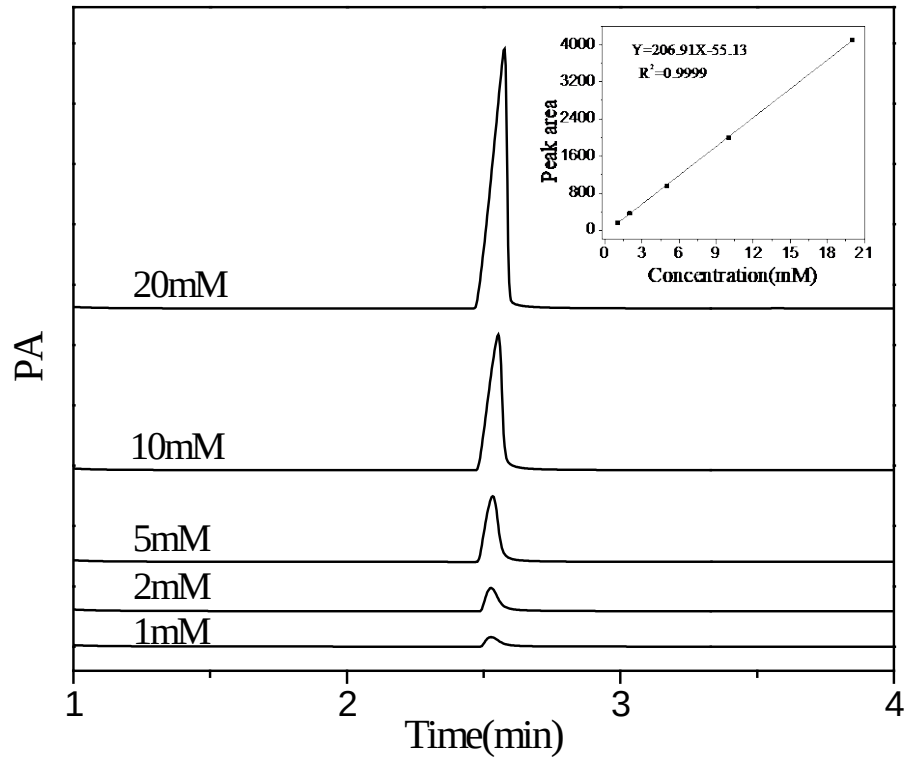

Fig. S18 Gas chromatograms (GC) of p-anisidine.

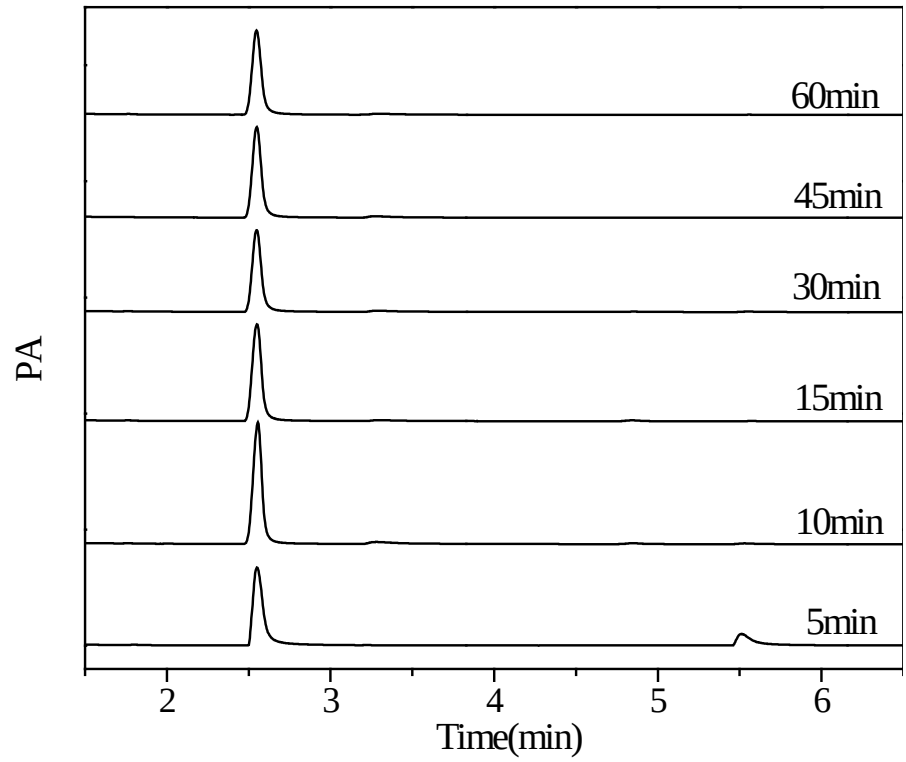

Fig. S19 The results of catalyst reaction for NaCas-Au NCs at different times.

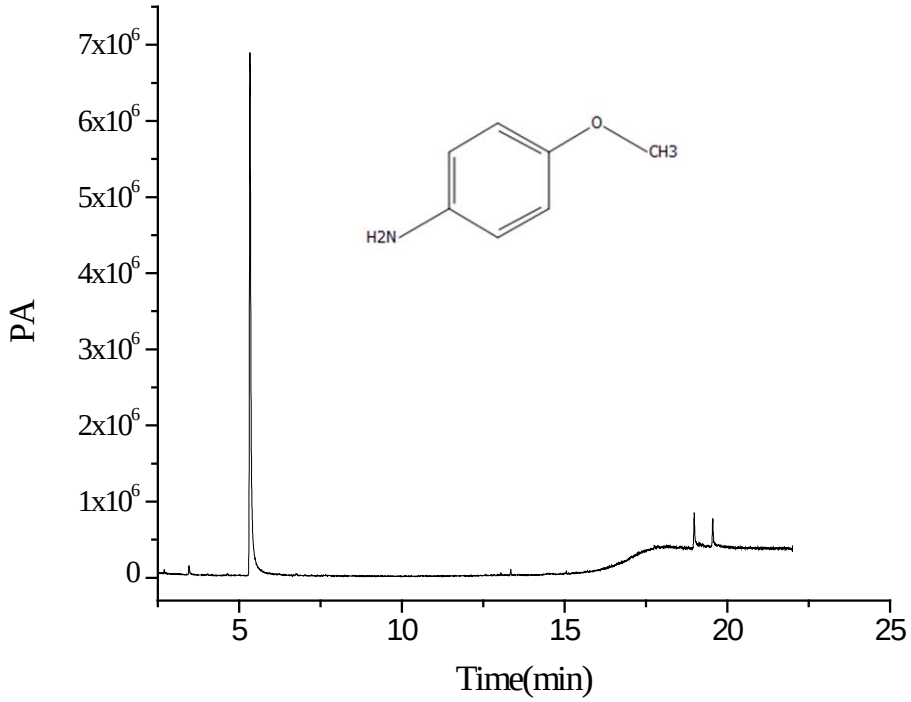

Fig. S20 Identification of catalytic product structure using GC-MS.

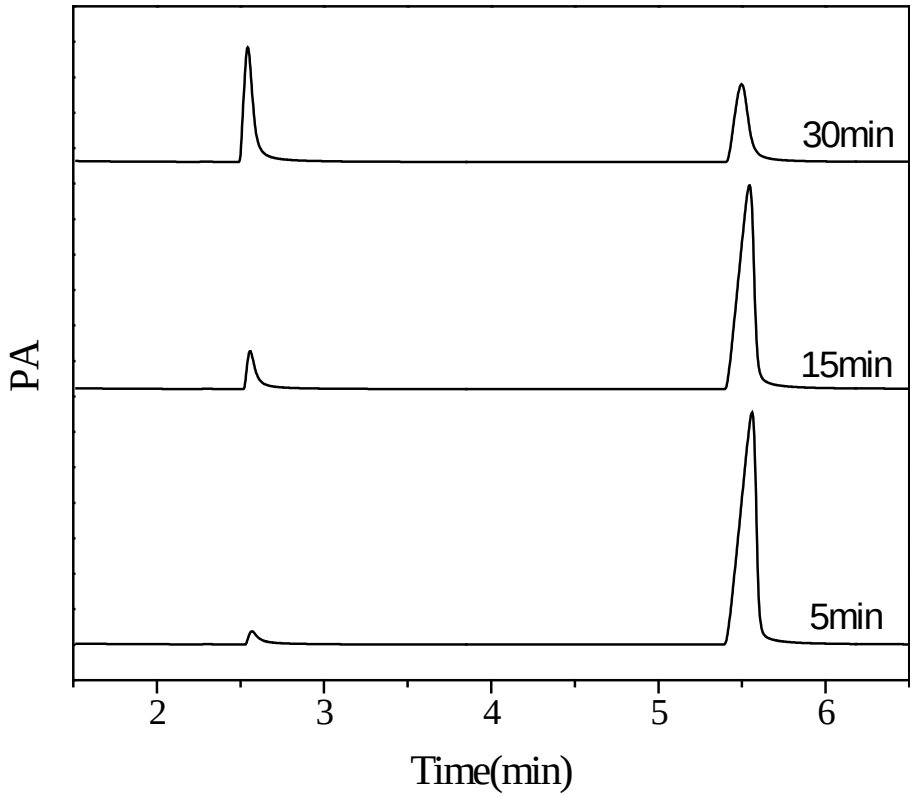

Fig. S21 The results of catalyst reaction for Au NPs at different times.

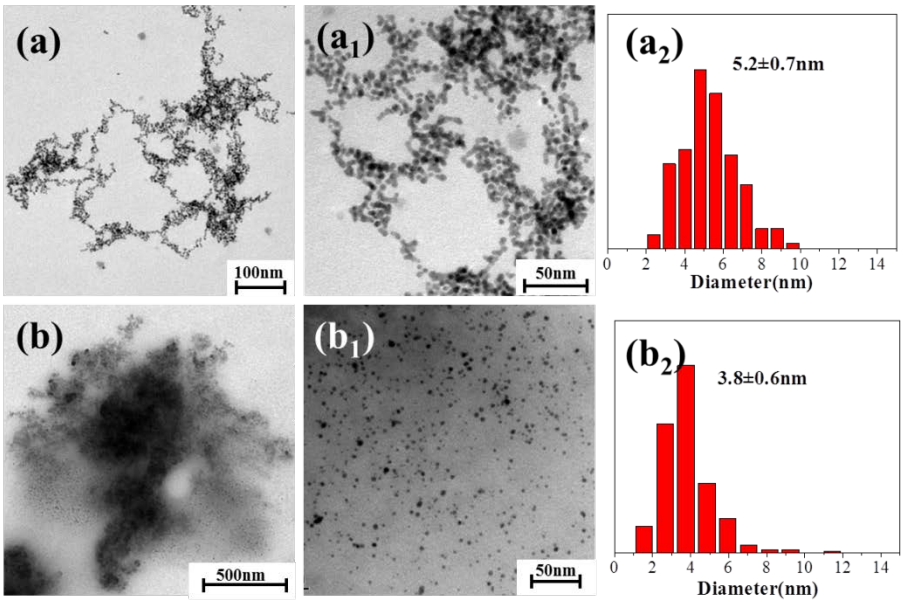

Fig. S22 (a, a_1) TEM of Au NPs, (a_2) diameter of Au NPs, (b, b_1) TEM of NaCas-Au NCs after demulsification 9th cycle, (b_2) diameter of Au in NaCas-Au NCs after 9th cycle.

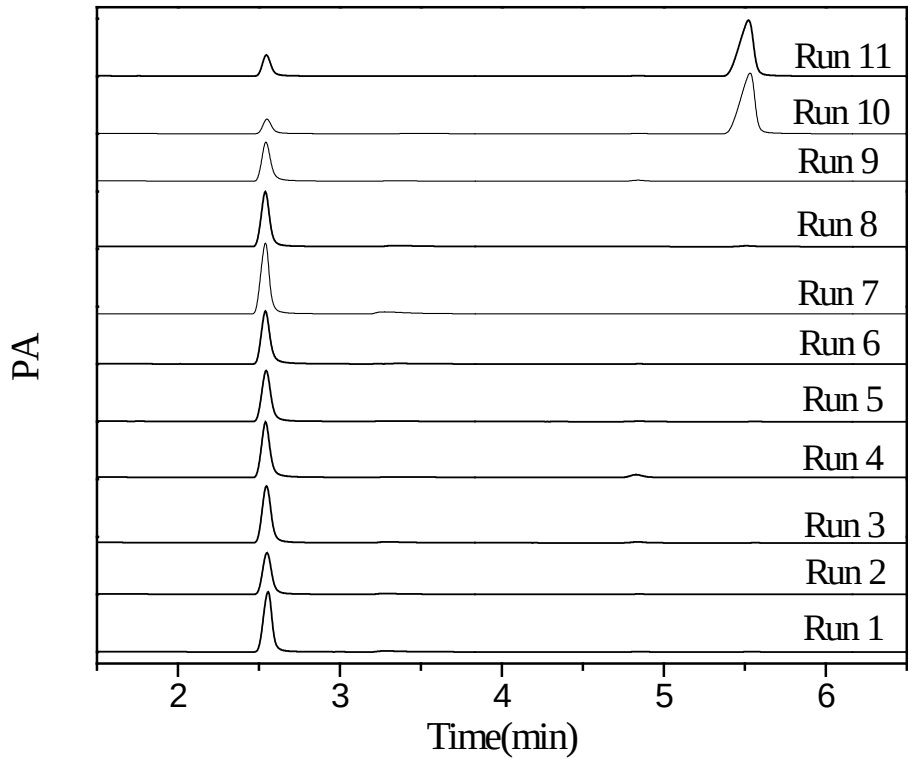

Fig. S23 The results of catalyst reaction for NaCas-Au NCs at different cycles.

Table S1. The conversion of catalyst reaction in sea water and saturated salt solution.

Catalyst	Solvent	Run1		Run2	
		Time/min	Yield/%	Time/min	Yield/%
NaCas-Au	Sea Water	20	83.25	20	81.88
NaCas-Au	Saturated NaCl	90	82.85	90	45.14

Table S2. The yield of catalyst reaction with different catalyst.

Catalyst	Run1		Run2	
	Time/min	Yield/%	Time/min	Yield/%
NaCas-Pd	60	78.69	60	68.22
NaCas-Rh	60	82.13	60	65.44

References

[1] Y. B. Chen, X. F. Zhu, T. X. Liu, W. F. Lin, C. H. Tang and R. Liu, *Food Hydrocolloids*, 2019, **87**, 404-412.

[2] C. Qi, J. Liu, Y. Jin, L. Xu, G. Wang, Z. Wang and L. Wang, *Biomaterials*, 2018, **163,** 89-104.

[3] D. Güzey, I. Gülseren, B. Bruce and J. Weiss, *Food Hydrocolloid*, 2006, **20**. 669-677.

[4] K. A. Mahmoud, K. B. Male, S. Hrapovic and J. H. Luong, *ACS Appl. Mater. Interfaces,* 2009, **1**, 1383-1386.

[5] C. G. De Kruif, T. Huppertz, V. S. Urban and A. V. Petukhov, Adv. *Colloid Interface Sci*., 2012, **171**, 36-52.

[6] K. J. Cross, N. L. Huq and E. C. Reynolds, *Biochemistry*, 2016, **55**, 4316-4325.

[7] T. Wang, X. Chen, Q. Zhong, Z. Chen, R. Wang and A. R. Patel, *Adv. Funct. Mater*., 2019, 1901830.

[8] S. Perego, E. Del Favero, P. De Luca, F. Dal Piaz, A. Fiorilli and A. Ferraretto, *Food Funct.*, 2015, **6**, 1796-1807.

[9] M. Ali Naqvi, K. Anaraki Irani, M. Katanishooshtari and D. Rousseau, *Curr. Protein Pept. Sci*., 2016, **17**, 368-379.

[10] V. A. Mittal, A. Ellis, A. Ye, P. J. Edwards and H. Singh, *Food Chem*., 2018, **239**, 17-22.

[11] D. D. Kitts, *Trends Food Sci. Tech*., 2005, **16**, 549-554.

[12] R. E. Reeves and N. G. Latour, *Science*, 1958, **128**, 472-472.

[13] K. J. Cross, N. L. Huq and E. C. Reynolds, *Biochemistry*, 2016, **55**, 4316−4325.

[14] X. Cui, J. Wang, B. Liu, S. Ling, R. Long and Y. Xiong, *J. Am. Chem. Soc.,* 2018, **140**, 16514-16520.

[15] Y. H. Kuan, R. Bhat and A. A. Karim, *J. Agric. Food chem.,* 2011, **59**, 4111-4118.